

## **Some Requirements for Electronic Properties of a Material for MHD: Thermal Emission of Electrons**

**P. Odier<sup>1</sup> and J. C. Rifflet<sup>1</sup>**

*Received December 30, 1980*

---

There have been significant advances in MHD (magnetohydrodynamics) conversion recently. However, the lifetime of electrodes remains too short due to degradation derived from several mechanisms. Electrical degradation is a consequence of an ionic conductivity contribution and of inefficient thermal emission of electrons. The last factor is analyzed for oxides. Point defects are important to understand the effect of the gaseous environment and influence mainly the preexponential term in electron emission expressions. A correlation between the electron affinity  $\chi$  and the band gap  $E_g$  may help to determine a rough value of  $\chi$ . Oxides with low electron affinity and appropriate doping appear attractive for further research.

---

**KEY WORDS:** Electron affinity; high temperature; magnetohydrodynamics; thermal emission of electrons; work function.

### **1. INTRODUCTION**

The durability of electrodes is a critical factor in the development of MHD (magnetohydrodynamics) technology. Electrode lifetime is limited by degradation imposed by the severe MHD environment. The major sources of degradation are classified according to three mechanisms in Fig. 1. Mechanical and chemical types will not be discussed, as considerable research has been devoted to these areas [1, 2]. In contrast, few reports [3-5] concern electrical degradation. In this work the results and discussion deal mainly with open-cycle MHD systems working at medium or high temperatures.

---

<sup>1</sup>Centre de Recherche sur la Physique des Hautes Températures, C.N.R.S., 45045 Orléans-Cedex, France.

<u>MECHANICAL</u>	- EROSION	GAS HIGH SPEED 1000ms <sup>-1</sup>   ASH
	- VAPORISATION	
	- THERMAL SHOCK	LOW THERMAL   CONDUCTIVITY
<u>CHEMICAL</u>	- SEED	K <sub>2</sub> CO <sub>3</sub>   KOH   CsOH
	- COAL SLAG ( LOW T MODE )	
	- VAPORISATION	
<u>ELECTRICAL</u>	- ELECTROLYSIS	
	- ARC AT ELECTRODES	

Fig. 1. Mechanisms of degradation for MHD electrodes.

## 2. ELECTRICAL DEGRADATION

Basically two mechanisms are involved in the electrical degradation of electrodes. Both are due to the flow of electrical current in the system. In the first, movement of electrical charges can generate electrolysis in the electrode. The second involves the transfer of charges from the electrode to the plasma. A very simple approach is given here.

### 2.1. Electrolysis

The electrical conductivity  $\sigma_T$  involves ionic and electronic contributions:

$$\sigma_T = \sigma_i + \sigma_e. \quad (1)$$

A high electronic transport number  $t_e = \sigma_e / \sigma_T$  is needed to avoid an excessive transport of matter by the current as shown in the following example. Let  $J_T$  be the total density of current; the number of monovalent ions carried through 1 cm<sup>2</sup> and during 1 s is

$$q_i = \frac{1}{1.6 \times 10^{-19}} (1 - t_e) J_T. \quad (2)$$

For a reasonable  $J_T = 1 \text{ A} \cdot \text{cm}^{-2}$ ,

$t_e$	0.5	0.9	0.99
$q_i$	$3 \times 10^{18}$	$6 \times 10^{17}$	$6 \times 10^{15}$

As about  $10^{22}$  ions are in  $1 \text{ cm}^3$ ,  $t_e > 0.99$  is needed for electrodes to ensure a long lifetime. When this is not the case, electrochemical reactions occur at the metal/oxide interface at the cathode but also at the oxide/plasma interface at the anode, causing irreversible degradation [4]. This was first recognized for ionic conductors constituted of oxides [6] in which reduction can be sufficient to develop metal inclusions. In addition, the absolute value of the electrical conductivity should be high and with a low activation energy [3] to avoid a large potential drop and Joule heating on the electrode. A reasonable lower limit for the electrical conductivity may be  $10^{-2} (\Omega \cdot \text{cm})^{-1}$ . Many studies [2–4, 7–9] concerning the electrical conductivity of electrodes have been reported, especially on multicomponent compounds, but will not be reviewed here.

## 2.2. Degradation by Arcs

As charges reach the cathode, they must be transferred to the plasma through several boundary layers generated mainly by temperature gradients between the electrodes and the hot plasma. Each of those layers is a source of inhomogeneity which decreases the specific power [10]. One source of inhomogeneity is the contact between the cold electrode and the hot plasma. To reduce the loss of power induced in this case, high-temperature electrodes are needed for a poorly dissociated plasma [11]. The reverse is true for a highly dissociated plasma ( $\text{O}_2$ -enriched gas mixture). The voltage drop can be high enough at the cathode or the anode to give rise to large electrical arcs which erode the electrodes and significantly limit their lifetime. This is probably one of the central problems in MHD. Research on the physics of arcs remains in progress, and many questions are not resolved [12]. However, some understanding of the process for degradation of metallic electrodes was recently obtained and applied to MHD conditions [13–16]. It may be assumed that at low surface temperatures the spot is constricted to a small area (very high current density) of the electrode. An increase in temperature lowers the current density (evolution to a diffuse mode of charge transfer). Finally, the erosion of relatively cold metallic electrodes is largely due to vaporization of the electrode locally heated to a very high temperature. Thermal emission of electrons is crucial in the erosion rate, which can be decreased by a factor of  $10^3$  by lowering the work function. Seed, K or Cs, is important as it is known to reduce the work function [17]. The effect of an oxidizing atmosphere on the erosion of metallic electrodes may be important

and should be studied [18]. An interesting attempt has been made by Bonet [18] using oxide cathodes to produce arcs in oxidizing conditions. Very little is known about erosion by arcs on oxide electrodes.

Several studies were made to avoid the arc regime or at least to control it. For example, an auxiliary arc helps to reduce the cathode voltage drop as demonstrated by Rostas [10]. The cathode also can be operated in a diffuse charge transfer mode for which critical conditions for the current density exist [19]. They depend mainly on the temperature, thermal properties of the electrode, and thermal emission of electrons.

In summary, the voltage drop at an electrode is responsible for the loss of specific power and the generation of arcs which limit the lifetime of electrodes. That voltage drop may, to a first approximation, be represented by

$$V = A_u Bl - V_e - J_0 \frac{l}{\sigma_g}, \tag{3}$$

where  $A$  is a geometric factor,  $u$  the velocity of the gas,  $l$  the interelectrode distance,  $B$  the magnetic strength (Fig. 2),  $V_e$  the voltage drop in the conducting electrode, and  $J_0 l / \sigma_g$  the contribution to the voltage drop of the plasma of conductivity  $\sigma_g \cdot J_0$  is the emitted current density at saturation. Equation (3) shows the importance of the electron emission in the MHD conversion limiting the current that the generator is able to deliver. A reasonable value of  $J_0$  is a few  $\text{A} \cdot \text{cm}^{-2}$ . Some remarks and results on  $J_0$  are given below.

### 3. THERMAL EMISSION OF ELECTRONS

#### 3.1. Basic Laws

It is appropriate to review here some of the fundamental laws used to describe the thermal emission of electrons. The density of the emitted current is given by the Richardson-Dushman equation:

$$J_0 = A_0 (1 - \bar{r}) T^2 \exp - \frac{\Phi}{kT}, \tag{4}$$

in which  $A_0 = 120 \text{ A} \cdot \text{cm}^{-2} \cdot \text{K}^{-2}$ ,  $\bar{r}$  is a mean thermoelectron reflection

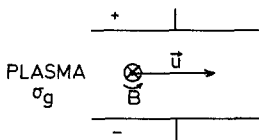


Fig. 2. Schematic representation of MHD conversion of electricity.

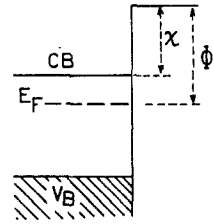


Fig. 3. Definition of the work function  $\Phi$  and of the electron affinity  $\chi$  for a semiconductor.

coefficient neglected below, and  $\Phi$  is the work function. The definition of  $\Phi$  is illustrated in Fig. 3, where CB and VB denote the conduction and valence band, and  $E_F$  is the Fermi level which can move in the forbidden gap of an oxide. In this case it is convenient to introduce  $\chi$ , the electron affinity, and  $n$ , the number of electrons in CB. Equation (4) is then written

$$J_0 = A_0 T^2 \frac{n}{N_c} \exp - \frac{\chi}{kT}, \tag{5}$$

in which  $N_c$  is the density of states in CB. With the help of Eq. (4) or (5) it is possible to calculate  $\Phi$  or  $\chi$  to meet the above-mentioned conditions for the

$$J \simeq 1 \text{ A}\cdot\text{cm}^{-2} \qquad \sigma \sim 10^{-2} (\Omega\cdot\text{cm})^{-1}$$

▪ METAL (Eq.(4))

	1500°C	1700°C
$\Phi$ (eV)	3.0	3.4

▪ OXIDE (Eq.(5),  $N_c = 4.8 \times 10^{15} T^{3/2} (\text{cm}^{-3})$   
 $\sigma = n_e \mu_e$ )

	$n_e$		$\mu_e$	
	1500°C			1700°C
$\chi$ (eV)	2.0	$6.10^{17}$	$10^{-1}$	2.3
	1.7	$6.10^{16}$	1	1.9
	1.3	$6.10^{15}$	10	1.5

Fig. 4. Electrical requirements for MHD electrodes.

electrical conductivity and the emitted current of an electrode. Calculations for two realistic temperatures of electrodes are shown in Fig. 4. This calculation is valid in vacuum for clean surfaces. The lower the temperature is, the lower the work function or electron affinity should be. In the case of an oxide, not only the electron affinity is important but also the electron concentration  $n$  and the electron mobility  $\mu_e$ .

In fact, as represented in Fig. 5, the collected current depends upon the applied voltage, the cathodic voltage in the case of MHD. In the space charge regime,  $J$  changes rapidly with  $V$  as  $V^{3/2}$ . When saturation is reached,  $J$  increases moderately following the Schottky law as  $\exp \alpha V^{1/2}/T$ . Extrapolation to zero field gives  $J_0$ . For high electrical fields ( $>10^5$  or  $10^6$  V · cm<sup>-1</sup>), the field emission controls the emission,  $J = hV^2 \exp - \beta/V$ .

Arcs can be generated depending on the surrounding gas, the emitted current, and the applied voltage. The actual regime in the MHD generator is not well known and may depend on the boundary layers controlling the cathodic voltage drop. It can be assumed, however, that the saturated range is achieved, as the electrical field is probably high at the electrode-plasma interface.

### 3.2. Measurements

The easiest way to measure the emitted current is to apply an electrical field high enough to be in the Schottky regime (see Fig. 5). Plotting  $\log J_0/T^2$  versus  $1/T$  leads to  $\Phi$  (at 0 K) by extrapolation.

For semiconductors, interesting measurements can be made at a constant temperature by varying  $n$ . Such studies have been performed for oxides at C.N.R.S. Orléans [20–22]. For these measurements the adjustable parameter is the oxygen pressure,  $P_{O_2}$ . Experiments are made in a high vacuum system in which pure oxygen is introduced ( $10^{-5}$ – $10^{-11}$  atm). The gas composition is controlled by a mass spectrometer.

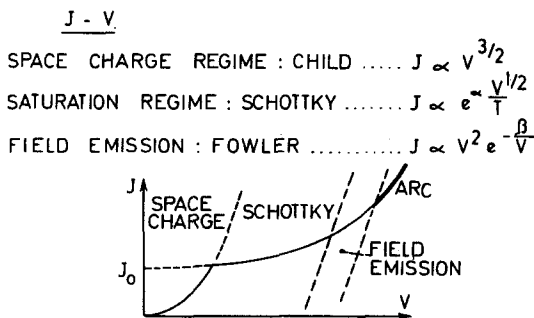


Fig. 5. Density of emitted current  $J$  versus applied voltage  $V$ .

Several ways to heat the samples may be used. A metallic wire (diameter, 0.25 mm) can be coated with the oxide [22] and heated directly by Joule heating. Small thickness of oxide (10–50  $\mu\text{m}$ ) are appropriate to avoid a radial gradient of  $T$ . Temperature is measured by optical pyrometry on the metallic wire (Fig. 6) with known emissivity. The cylindrical geometry with guard anodes is useful to define correctly the emitting area of the cathode and to obtain  $J_0$ . The use of iridium wire permits work at high temperatures even in the presence of oxygen ( $10^{-5}$  atm maximum in these experiments). For very high temperatures, another configuration is preferred [23]. We use an imaging technique shown in Fig. 7. The light of a xenon lamp is focused on a sample by elliptical mirrors, the sample being under vacuum inside a quartz bubble. The anode is a platinum wire positioned a few millimeters from the cathode. A special arrangement (see Fig. 7) is made to measure the temperature. A modulator is rotated and the pyrometer sees the radiating sample when the lamp is off. The frequency is adjusted to the thermal conductivity of the sample and to the time constant of the pyrometer. The shutter is open a few milliseconds and small decreases in temperature ( $\approx 10^\circ\text{C}$ ) are observed; the emitted current is simultaneously recorded. Very high temperatures can be achieved with such a system and the melting temperature of  $\text{Al}_2\text{O}_3$  was found in good agreement with that of previous works [25].

### 3.3. Experimental Results for Oxides: Variation of $n$ with $P_{\text{O}_2}$

Oxides are important because of their high stability under various conditions. Some of our results are summarized below. In general, oxides equilibrated with oxygen are well described by point defect theories [26]. It can be easily demonstrated that  $n \propto P_{\text{O}_2}^{-1/z}$ , where  $z$  depends on the point

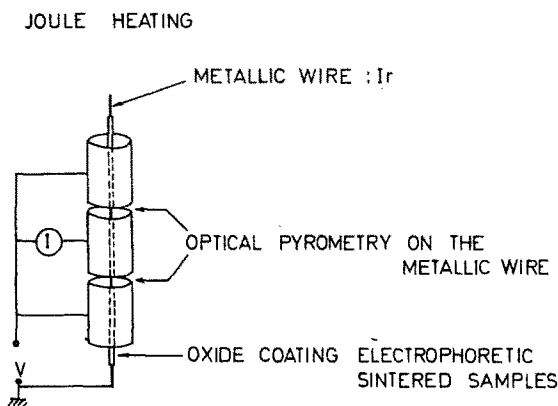


Fig. 6. Schematic representation of the measurement of electron emission by the Joule heating method.

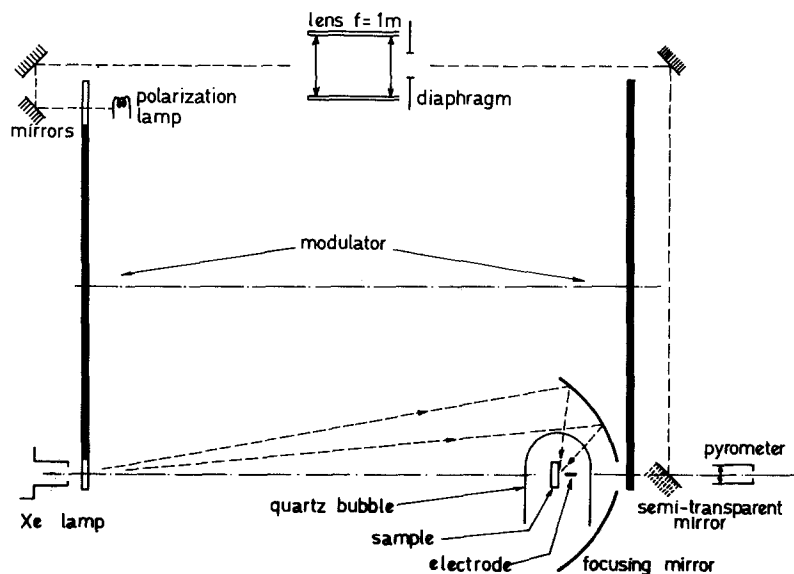
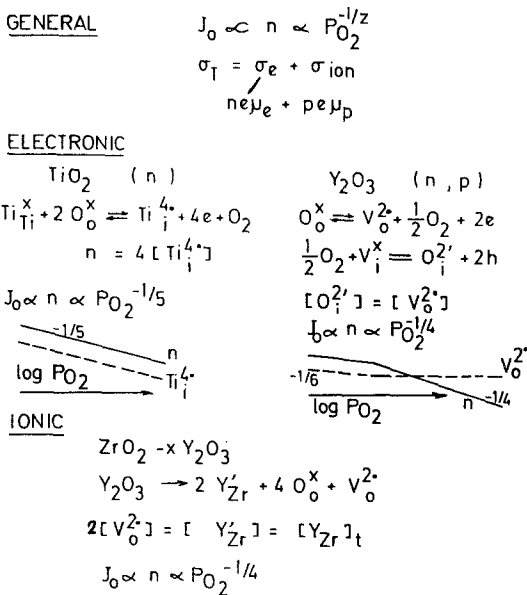


Fig. 7. Schematic representation of the measurement of electron emission at high temperatures.

defect [22, 26]. Following the variation of  $J_0$  with  $P_{O_2}$  gives direct information on the variation of  $n$  [Eq. (5)]. This is a great advantage with respect to the electrical conductivity in which several charge carriers and mobilities are involved [Eq. (1)]. Figure 8 summarizes the various results obtained on very different systems.  $TiO_2$  and  $Y_2O_3$  are both electronic conductors but  $TiO_2$  is  $n$  type in the experimental range [27].  $Y_2O_3$  changes from an  $n$  type to a  $p$  type. In both cases,  $J_0$  follows very well the predicted law. The electron affinity is about 4 eV for  $TiO_2$  [28] and 2 eV for  $Y_2O_3$  [22]. The ionic electrolyte  $ZrO_{2-x}Y_2O_3$  (solid solution) is interesting because it is possible here to follow the variation of  $n$  with  $P_{O_2}$  without measuring the electronic conductivity which is actually more than 3 orders of magnitude lower than the total conductivity:  $n$  varies as  $P_{O_2}^{-1/4}$ , as expected [29]. Emission of electrons is thus a new method to study minority defects in oxides. The electron affinity of stabilized zirconia is in agreement with previous values obtained for pure zirconia (3 eV) [20].

Alumina is a very interesting material used in several high-temperature devices.  $Al_2O_3$  emits electrons, and this has been recognized to be the reason for impedance leakage in high-resistance measurements at elevated temperatures [30–32]. Until now the thermal emission of electrons from alumina has not been investigated in detail. We recently obtained new results for commercial alumina (99.7%). Good agreement was obtained by two heating methods: Joule and radiation. The emitted current displayed a very unexpected behavior. No change of  $J_0$  with  $P_{O_2}$  (Fig. 9) is observed except in the high  $P_{O_2}$ ,





**ABSOLUTE COMPARISON OF EMITTED CURRENT**

T = 1700 °C      P<sub>O<sub>2</sub></sub> = 10<sup>-6</sup> atm.

	ZrO <sub>2</sub>	Al <sub>2</sub> O <sub>3</sub>	TiO <sub>2</sub>	ZrO <sub>2</sub> -Y <sub>2</sub> O <sub>3</sub>	Y <sub>2</sub> O <sub>3</sub>
J (Acm <sup>-2</sup> )	10 <sup>-5</sup> 10 <sup>-4</sup>	10 <sup>-4</sup> 10 <sup>-3</sup>	10 <sup>-4</sup> 10 <sup>-3</sup>	10 <sup>-4</sup> 10 <sup>-3</sup>	10 <sup>-2</sup> 10 <sup>-1</sup>

**Fig. 8.** Variations of *n* and *J*<sub>0</sub> with *P*<sub>O<sub>2</sub></sub> and comparison of the emitted current for several oxides.

range, where a slow decrease is apparent. Such variations of *n* with *P*<sub>O<sub>2</sub></sub> are typical of an impurity-controlled mechanism [33]. The work function of commercial alumina is about 4.7 eV and depends on the type of major impurity [24]. As compared in Fig. 8, emission of Al<sub>2</sub>O<sub>3</sub> is not low, and it may be asked, Is Al<sub>2</sub>O<sub>3</sub> an insulator if it emits electrons? These experiments demonstrate the importance of measurements of emission of electrons at high temperatures.

**3.4. Absolute Values of the Emitted Current: The Electron Affinity**

As indicated above, a high emission is needed for a material to be used in an MHD generator. Due to favorable properties (Fig. 8), Y<sub>2</sub>O<sub>3</sub> may be considered: σ<sub>Y<sub>2</sub>O<sub>3</sub></sub>(1700°C) ≈ 10<sup>-2</sup> (Ω · cm)<sup>-1</sup>, *J*<sub>Y<sub>2</sub>O<sub>3</sub></sub>(1700°C) ≈ 10<sup>-1</sup> A · cm<sup>-2</sup>. Equation (5) shows that the sensitive parameter is the electron affinity χ.

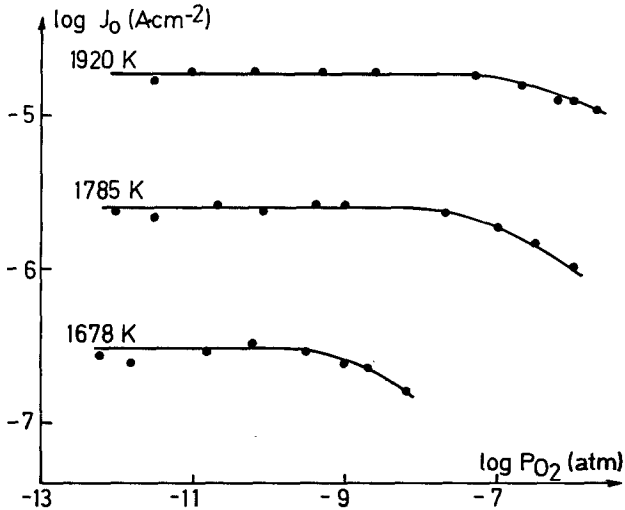


Fig. 9. Electron emission for commercial alumina (99.7%) at various oxygen pressures.

This is a very poorly known constant, as direct measurements of  $\chi$  have not been made. Recently, increasing interest has been given to electron affinity as an important factor for solar photovoltaic [34, 35] and photoelectrochemical cells [36]. Empirical correlations may help to select a material given the lack of experimental data. Since 1974, some success has been achieved using the work of Nethercot [37]. He has assumed that the electronegativity (EN) of a compound AB is the geometric mean of the Mulliken EN for the individual atoms:  $EN(AB) = EN_A \cdot EN_B)^{1/2}$ . He has also postulated that  $EN(AB) = E_F^i$ , where  $E_F^i$  is the intrinsic Fermi energy. Hence, this provides a very simple way for calculating  $\chi$  in compounds with an energy gap  $E_g$ :

$$\chi = EN(AB) - \frac{1}{2} E_g. \quad (6)$$

The EN of individual atoms,  $EN = 1/2(A + I)$ , may be calculated using values of atomic electron affinity [38]  $A$  and of first ionization potential [39]  $I$  of elements.

Butler and Ginley [40, 41] have calculated the electron affinities of various oxides using this procedure. Some results are given in Table I. They should be used with caution and to select a material in qualitative fashion. It is beyond the scope of this work to criticize these values, as only general

Table I. Calculated Values of Electron Affinity of Oxides<sup>a</sup>

Oxide	Electron affinity (eV)	Band gap (eV)
MgO	1.4	7.8
CaO	0.9	7.7
SrO	1.8	5.7
BaO	1.9	5.1
Sc <sub>2</sub> O <sub>3</sub>	2.4	6.0
Y <sub>2</sub> O <sub>3</sub>	2.5	5.6
La <sub>2</sub> O <sub>3</sub>	4.1	2.3
TiO <sub>2</sub>	4.3	3.0
ZrO <sub>2</sub>	3.4	5.0
HfO <sub>2</sub>	3.1	5.5
NiO	3.9	3.7
ZnO	4.2	3.3
Al <sub>2</sub> O <sub>3</sub>	0.4	9.9
SiO <sub>2</sub>	0.9	11.0

<sup>a</sup>Calculated using Eq. (6) and values of  $E_g$  and EN given in Refs. 42 and 43.

conclusions are of interest. An important point, however, is that  $\chi$  decreases when the gap increases, Fig. 10. Since the valence band is formed by O(2p) levels which will be at nearly the same energy for all the oxides, decreasing the electron affinity corresponds to increasing the band gap [36, 44]. The ultimate situation is for alumina, which has a very high energy gap (10 eV). A low electron affinity is expected;  $\chi = 1$  eV seems reasonable [45, 46].

In conclusion, on one hand, Y<sub>2</sub>O<sub>3</sub> would be a good candidate for electrode material because it has a relatively small gap and a small  $\chi$ ; on the other hand, attempts to use the low electron affinity of wide-gap oxides seem promising. In this respect, doping of alumina with appropriate donors is attractive.

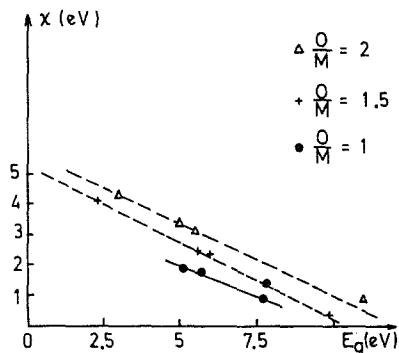


Fig. 10. Electron affinity of different oxides versus band gap. O/M represents the ratio of oxygen/metal of the oxide.

#### 4. CONCLUSION

Most studies on electrical properties of electrodes for MHD deal with electrical conductivity. However, the emission of electrons is a crucial parameter in the electrical degradation of materials. Studies of the thermal emission of electrons are imperative in material studies for MHD electrodes. An attractive way to find efficient emitters is to dope oxides having low electron affinities.

#### REFERENCES

1. A. Kantrowitz, *Conference on High Temperature Science Related to Open-Cycle Coal-Fired MHD Systems* (Argonne National Laboratory, Argonne, Illinois, 1977), p. 289.
2. T. Sata and M. Yoshimura, *Zairyo Kagaku* **15**(2):87 (1978).
3. B. R. Rossing and H. K. Bowen, *Critical Material Problems in Energy Production* (Academic Press, New York, 1976), Chap. 11.
4. J. Hizusaki, W. R. Cannon, and H. K. Bowen, *J. Am. Ceram. Soc.* **63**(7,8):391 (1980).
5. A. M. Anthony, *Rev. Int. Htes. Temp. Refract.* **13**:230 (1976).
6. J. Millet and D. Yerouchalmi, *La Production d'Electricité par Conversion Magnétohydrodynamique* (Technip, Paris, 1967).
7. W. R. Cannon, M. Yoshimura, J. Mizusaki, T. Sasamoto, R. I. Pober, J. Hart, H. K. Bowen, J. F. Louis, *Proceedings of the 17th Symposium on the Engineering Aspect of MHD*, C. H. Kruger, ed. (Stanford University, Stanford, Calif., 1978), G.5.1–G.5.6.
8. L. P. Domingues, T. Negas, A. J. Armstrong, and W. R. Hosler, *Proceedings of the 17th Symposium on the Engineering Aspect of MHD*, C. H. Kruger, ed. (Stanford University, Stanford, Calif., 1978), G.6.1–G.6.5.
9. H. N. King, G. Murphy, K. M. Castelliz, M. Manuel, and M. Rocknell, *Rev. Int. Htes. Temp. Refract.* (in press).
10. F. Rostas, *Rev. Gen. Electr.* **1**(12):983 (1965).
11. A. V. Bagdonas, V. A. Bashilov, V. L. Bobrov, and Yu. V. Makarov, *Teplofizika Vysokikh Temp.* **16**(2):438 (1978).
12. E. Pfender, *Gaseous Electronics* (Academic Press, New York, 1978), Vol I, Chap. 5.
13. I. I. Bielis, *Teplofizika Vysokikh Temp.* **16**(4):848 (1978).
14. I. I. Bielis, *Teplofizika Vysokikh Temp.* **15**(6):1269 (1977).
15. I. I. Bielis, *Teplofizika Vysokikh Temp.* **15**(5):965 (1977).
16. I. I. Bielis, V. I. Zalkind, and A. S. Tikhotskii, *Teplofizika Vysokikh Temp.* **15**(1):158 (1977).
17. N. S. Rasor and C. Warner, *J. Appl. Phys.* **35**(9):2589 (1964).
18. C. Bonet, 4th Int. Symp. Plasma Chem. Invited Lecture, Zürich, Aug. (1979).
19. A. M. Virnik, N. H. Zykova, T. S. Kurakina, and E. V. Mel'nikov, *Teplofizika Vysokikh Temp.* **15**(6):1148 (1977).
20. J. P. Loup and A. M. Anthony, *Phys. Status Solidi A* **38**:499 (1970).
21. J. C. Rifflet, P. Odier, J. P. Loup, and A. M. Anthony, *J. Am. Ceram. Soc.* **58**(11–12):493 (1975).
22. P. Odier and J. P. Loup, *J. Solid State Chem.* **34**:107 (1980).
23. J. C. Rifflet, P. Odier, J. P. Loup, M. Hoch, and A. M. Anthony, *Rev. Int. Htes. Temp. Refract.* **16**(4):444 (1979).
24. J. C. Rifflet, Thèse (Orléans, France, 1981).
25. Recommended value of IUPAC (1970),  $2054 \pm 6^\circ\text{C}$ ; observed value,  $2040 \pm 10^\circ\text{C}$ .
26. F. A. Kröger, *The Chemistry of Imperfect Crystals*, 3rd ed. (North Holland, Amsterdam, 1974).

27. J. F. Baumard and E. Tani, *Phys. Status Solidi A* **39**:373 (1979).
28. P. Odier, unpublished results.
29. P. Odier and A. M. Anthony, *Ann. Chim. Sci. Mater.* **4**:499 (1979).
30. J. P. Loup and A. M. Anthony, *Rev. Int. Htes. Temp. Refract.* **1**:15 (1964).
31. J. P. Loup and A. M. Anthony, *Rev. Int. Htes. Temp. Refract.* **1**:193 (1964).
32. D. W. Peters, L. Feinstein, and C. Peltzer, *J. Chem. Phys.* **42**(7):2345 (1965).
33. S. K. Mohapatra, S. K. Tiku, and F. A. Kröger, *J. Am. Ceram. Soc.* **62**(1-2): 50 (1979).
34. R. Singh and J. Shewchun, *J. Appl. Phys. Lett.* **33**(7):601 (1978).
35. H. Schoijet, *Solar Energy Mater.* **1**:43 (1979).
36. H. A. Butler and D. S. Ginley, *J. Mater. Sci.* **15**:1 (1980).
37. A. H. Nethercot, *Phys. Rev. Lett.* **33**(18):1088 (1974).
38. H. Hotop and W. C. Lineberger, *J. Phys. Chem. Ref. Data* **4**(3):539 (1975).
39. D. E. Gray (ed.), *American Institute of Physics, Handbook*, 2nd ed. MacGraw-Hill, New York, 1954).
40. M. A. Butler and D. S. Ginley, *J. Electrochem. Soc.* **125**:228 (1978).
41. D. S. Ginley and M. A. Butler, *J. Electrochem. Soc.* **125**:1968 (1978).
42. N. H. Stehlon and E. L. Cook, *J. Phys. Chem. Ref. Data* **2**(1):163 (1973).
43. H. B. Michaelson, *IBM J. Res. Dev.* **22**(1):72 (1978).
44. H. H. Kung, H. S. Jarrett, A. N. Sleight, and A. Ferretti, *J. Appl. Phys.* **48**:2463 (1977).
45. C. R. Viswanathan and R. Y. Loo, *Appl. Phys. Lett.* **21**(8):370 (1972).
46. Yu. I. Semov, *Phys. Status Solidi* **32**:K41 (1969).